Wave based modeling of structure-borne sound transmission in finite sized double walls

A. Dijckmans[1,2]
[1]KU Leuven, Department of Civil Engineering, Kasteelpark Arenberg 40, B-3001 Leuven, Belgium
[2]Acoustics Research Unit, School of Architecture, University of Liverpool, Liverpool L69 7ZN, UK

Summary
In this paper, a wave based model is used for the investigation of the sound transmission through double walls with structural connections. Point and line connections with an increasing degree of complexity are introduced in the double wall model to incorporate the effect of structure-borne paths. The studs and ties are modeled as rigid connections or a combination of translational and rotational springs. Alternatively, the studs are modeled as beams, accounting for the modal behaviour of the studs. The wave based results are compared with experiments and infinite plate models based on a decoupled approach or a periodic approach. It is shown that the finite dimensions can have a significant influence on the sound insulation, both at low frequencies and at higher frequencies. The pass- and stop-band behaviour of periodic structures cannot fully develop in finite double walls.

PACS no. 43.55.Rg, 43.55.Ti, 43.55.Ka

1. Introduction

The acoustic performance of double leaf walls is often determined by structure-borne sound transmission through mechanical links between the two leaves, like studs or ties. The transmission loss of double panels with structural links has been studied extensively, both experimentally and theoretically.

Hongisto *et al.* [1] carried out a comprehensive experimental parametric study of double walls. For double walls with studs, the stiffness or type of the stud and the spacing of the screws between the panel and the stud were the most influencing parameters.

Structural coupling can be simply introduced in SEA models as a coupling loss factor between the plates [2]. Semi-analytical prediction models [3, 4, 5] address the sound transmission through double walls with structural links by decoupling the total transmission in terms of an airborne path through the cavity and a structure-borne path through the structural links, under the assumption of infinite plates and diffuse incident sound fields. A second type of analytic models assume infinite structures with periodically placed studs [6, 7, 8]. The periodicity of the structure allows the use of Fourier transform techniques to solve the problem in the wavenumber domain.

Assumptions made in the analytic and statistical models, like high modal density and modal overlap, are often not satisfied in laboratory and real conditions. Previously, a wave based model has been developed to model the airborne sound transmission through double walls between two rooms, taking into account the modal behaviour of both rooms and structure [9]. It was shown that the modal behaviour of the double wall can play an important role in a broad frequency range. In this paper, the sound transmission through finite double walls with structural point or line connections is investigated. Relatively few studies treating this problem have been reported in literature. Díaz-Cereceda *et al.* [10] used modal analysis to predict the vibration level difference between coupled plates in the case of mechanical excitation. Arjunan *et al.* [11] developed a finite element model for gypsum plasterboard walls with steel studs. Due to the high computational cost, calculations were only performed at the 1/3 octave band center frequencies. The computational efficiency of the wave based model allows a more detailed analysis of the transmission loss over frequency, which is important when the fluctuations due to the modal behaviour are large.

2. Wave based model (WBM)

2.1. Problem definition

Figure 1 gives a schematic overview of the model. A rectangular double wall is placed between two rooms with rigid side and back walls. A harmonic volume point source is placed in the source room to calculate the sound transmission through the double wall.

(c) European Acoustics Association

Copyright© (2015) by EAA-NAG-ABAV, ISSN 2226-5147
All rights reserved

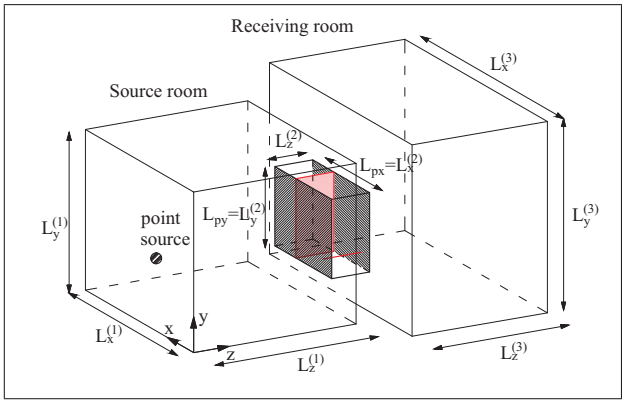

Figure 1. Geometry of the wave based model: a double panel with structural point and line connections, placed between two rooms with rigid side and back walls.

Flanking transmission is neglected. The plates have simply supported boundary conditions and are assumed homogeneous, isotropic and acoustically thin. The two plates are connected by N_s point connections and N_l vertical line connections. Horizontal line connections are not considered in this paper but can be taken into account in a similar way. The point and line connections are modeled as massless rigid or massless spring connections. Alternatively, a beam model is used for the line connections.

2.1.1. Rooms and air cavity

The source room is divided into two subdomains ($V^{(0)}$ and $V^{(1)}$) by a plane through the point source, parallel to the back wall. It is assumed that the structural connections in the cavity ($V^{(2)}$) of the double wall are acoustically transparent, i.e. they do not block the acoustic waves in the cavity. The steady-state acoustical pressure $\underline{p}_a^{(i)}$ in each (sub)room $V^{(i)}$ $(i = 0 \ldots 3)$ is governed by the homogeneous Helmholtz equation:

$$\nabla^2 \underline{p}_a^{(i)} + k_a^2 \underline{p}_a^{(i)} = 0. \tag{1}$$

$k_a = \frac{\omega}{c_a}$ is the acoustic wave number in air, with ω the circular frequency and c_a the speed of sound in air. The underscore (_) denotes a complex value throughout the paper. In source and receiving room, uniform spatial damping is introduced by making the acoustic wave number complex:

$$\underline{k}_a^{(i)} = k_a \left(1 - j \frac{1}{2} \frac{2.2}{f T^{(i)}}\right), \tag{2}$$

where $T^{(i)}$ is the reverberation time of the room. f is the frequency, $j = \sqrt{-1}$.

2.1.2. Rigid and spring connections

Each point connection $(i = 1 \ldots N_\mathrm{s})$ is modeled as a massless translational spring with a stiffness $K_{\mathrm{t}i}$. The stiffness links the force $\underline{F}_{\mathrm{s}i}$ in the spring to the displacement of the two panels at the connection:

$$\underline{w}_p^{(1)}(x_{\mathrm{s}i}, y_{\mathrm{s}i}) - \underline{w}_p^{(2)}(x_{\mathrm{s}i}, y_{\mathrm{s}i}) = \frac{\underline{F}_{\mathrm{s}i}}{K_{\mathrm{t}i}}, \tag{3}$$

with $(x_{\mathrm{s}i}, y_{\mathrm{s}i})$ the position of point connection i.

Each line connection $(i = 1 \ldots N_\mathrm{l})$ is modeled as a combination of a massless translational spring with stiffness per unit length $K'_{\mathrm{t}i}$ and a massless rotational spring with stiffness per unit length $K'_{\mathrm{r}i}$. The force $\underline{F}_{\mathrm{l}i}(y)$ and moment $\underline{M}_{\mathrm{l}i}(y)$ per unit length for each line connection i are linked to the displacement and rotation of the two panels at the line connection by:

$$\underline{w}_p^{(1)}(x_{\mathrm{l}i}, y) - \underline{w}_p^{(2)}(x_{\mathrm{l}i}, y) = \frac{\underline{F}_{\mathrm{l}i}(y)}{K'_{\mathrm{t}i}}, \tag{4}$$

$$\frac{\partial \underline{w}_p^{(1)}(x_{\mathrm{l}i}, y)}{\partial x} - \frac{\partial \underline{w}_p^{(2)}(x_{\mathrm{l}i}, y)}{\partial x} = \frac{\underline{M}_{\mathrm{l}i}(y)}{K'_{\mathrm{r}i}}, \tag{5}$$

with $x_{\mathrm{l}i}$ the position of vertical line connection i.

Rigid point and line connections can be incorporated in a straightforward way by setting the compliances $C_{\mathrm{t}i} = 1/K_{\mathrm{t}i}$, $C'_{\mathrm{t}i} = 1/K'_{\mathrm{t}i}$ and $C'_{\mathrm{r}i} = 1/K'_{\mathrm{r}i}$ equal to zero.

2.1.3. Beams

For beams with a symmetric section, the translational displacement $\underline{w}_{\mathrm{b}zi}$ and rotational displacement $\underline{\theta}_{\mathrm{b}yi}$ of each beam $(i = 1 \ldots N_\mathrm{l})$ are governed by following uncoupled equations:

$$\left[\underline{B}_{\mathrm{b}i} \frac{\partial^4}{\partial y^4} - \omega^2 m'_{\mathrm{b}i}\right] \underline{w}_{\mathrm{b}zi} = \underline{F}_{\mathrm{l}i}^{(1)} - \underline{F}_{\mathrm{l}i}^{(2)}, \tag{6}$$

$$\left[\underline{W}_{\mathrm{b}i} \frac{\partial^4}{\partial y^4} + \underline{T}_{\mathrm{b}i} \frac{\partial^2}{\partial y^2} - \omega^2 I_{\mathrm{bS}i}\right] \underline{\theta}_{\mathrm{b}yi} = \underline{M}_{\mathrm{l}i}^{(1)} - \underline{M}_{\mathrm{l}i}^{(2)}. \tag{7}$$

$\underline{F}_{\mathrm{l}i}^{(1)}$ and $\underline{M}_{\mathrm{l}i}^{(1)}$ are the force and moment per unit length exerted by plate 1 on the beam. $\underline{F}_{\mathrm{l}i}^{(2)}$ and $\underline{M}_{\mathrm{l}i}^{(2)}$ are the force and moment exerted by plate 2. The beam bending stiffness $\underline{B}_{\mathrm{b}i}$, torsional stiffness $\underline{T}_{\mathrm{b}i}$ and warping stiffness $\underline{W}_{\mathrm{b}i}$ are defined as

$$\underline{B}_{\mathrm{b}i} = E_{\mathrm{b}i}(1 + j\eta_{\mathrm{b}i}) I_{xi}, \tag{8}$$

$$\underline{T}_{\mathrm{b}i} = G_{\mathrm{b}i}(1 + j\eta_{\mathrm{b}i}) J_{yi}, \tag{9}$$

$$\underline{W}_{\mathrm{b}i} = E_{\mathrm{b}i}(1 + j\eta_{\mathrm{b}i}) I_{wi}, \tag{10}$$

with I_{xi} the second moment of area with respect to the x-axis, J_{yi} the torsional constant in the y-direction and I_{wi} the warping constant. $m'_{\mathrm{b}i}$ is the mass per unit length and $I_{\mathrm{bS}i}$ the moment of inertia per unit length of beam i. The material of beam i has a Young's modulus $E_{\mathrm{b}i}$, a shear modulus $G_{\mathrm{b}i}$ and a loss factor $\eta_{\mathrm{b}i}$.

2.1.4. Plates

The transverse displacements $\underline{w}_p^{(i)}$ of the plates $(i = 1, 2)$ fulfil Kirchhoff's thin plate bending wave equa-

tion:

$$\left[\underline{B}_1'\nabla^4 - \omega^2 m_1''\right]\underline{w}_p^{(1)} = \underline{p}_a^{(1)} - \underline{p}_a^{(2)} - \sum_{i=1}^{N_\mathrm{s}}\left[\underline{F}_{\mathrm{s}i}\delta(x-x_{\mathrm{s}i}, y-y_{\mathrm{s}i})\right] - \sum_{i=1}^{N_\mathrm{l}}\left[\underline{F}_{\mathrm{l}i}^{(1)}\delta(x-x_{\mathrm{l}i}) - \frac{\partial}{\partial x}\underline{M}_{\mathrm{l}i}^{(1)}\delta(x-x_{\mathrm{l}i})\right], \quad (11)$$

$$\left[\underline{B}_2'\nabla^4 - \omega^2 m_2''\right]\underline{w}_p^{(2)} = \underline{p}_a^{(2)} - \underline{p}_a^{(3)} + \sum_{i=1}^{N_\mathrm{s}}\left[\underline{F}_{\mathrm{s}i}\delta(x-x_{\mathrm{s}i}, y-y_{\mathrm{s}i})\right] + \sum_{i=1}^{N_\mathrm{l}}\left[\underline{F}_{\mathrm{l}i}^{(2)}\delta(x-x_{\mathrm{l}i}) - \frac{\partial}{\partial x}\underline{M}_{\mathrm{l}i}^{(2)}\delta(x-x_{\mathrm{l}i})\right], \quad (12)$$

where the plate bending stiffness $\underline{B}_i'$ is defined as

$$\underline{B}_i' = \frac{E_i h_i^3(1+j\eta_i)}{12(1-\nu_i^2)}. \quad (13)$$

$m_i'' = \rho_i h_i$ is the surface mass density and h_i the thickness of plate i. The material of plate i has a density ρ_i, a Young's modulus E_i, a loss factor η_i and a Poisson's ratio ν_i. The equations of motion account for the fluid loading and the forces and moments exerted by the point and line connections. In the case of rigid or spring connections, the forces and moments exerted on plate 1 and plate 2 are the same: $F_{\mathrm{l}i}^{(1)} = F_{\mathrm{l}i}^{(2)} = F_{\mathrm{l}i}$ and $M_{\mathrm{l}i}^{(1)} = M_{\mathrm{l}i}^{(2)} = M_{\mathrm{l}i}$.

2.2. Field variable expansions

The acoustic pressures are approximated in terms of the following acoustic wave function expansion,

$$\underline{\hat{p}}_a^{(i)} = \sum_{m,n}\left[e^{-j\underline{k}_{z,mn}^{(i)}z}\underline{P}_{mn}^{(i)} + e^{j\underline{k}_{z,mn}^{(i)}z}\underline{Q}_{mn}^{(i)}\right] \times \cos\left(\frac{m\pi}{L_x^{(i)}}x\right)\cos\left(\frac{n\pi}{L_y^{(i)}}y\right), \quad (14)$$

where

$$\underline{k}_{z,mn}^{(i)} = \sqrt{\left(\underline{k}_a^{(i)}\right)^2 - \left(\frac{m\pi}{L_x^{(i)}}\right)^2 - \left(\frac{n\pi}{L_y^{(i)}}\right)^2}, \quad (15)$$

with m, n = 0,1,2,.... The wave functions are exact solutions of the homogeneous Helmholtz equation. The time dependence $e^{j\omega t}$ has been omitted throughout this paper.

Using Euler's equation, eq. (14) leads to following wave function expansion for the air particle displacement in the z-direction,

$$\underline{\hat{w}}_a^{(i)} = \frac{-j}{\omega^2\rho_a}\sum_{m,n}\left[e^{-j\underline{k}_{z,mn}^{(i)}z}\underline{P}_{mn}^{(i)} - e^{j\underline{k}_{z,mn}^{(i)}z}\underline{Q}_{mn}^{(i)}\right] \times \underline{k}_{z,mn}^{(i)}\cos\left(\frac{m\pi}{L_x^{(i)}}x\right)\cos\left(\frac{n\pi}{L_y^{(i)}}y\right), \quad (16)$$

with ρ_a the density of air.

The transverse displacement of the acoustically thin plates is written as an expansion series:

$$\underline{\hat{w}}_p^{(i)} = \sum_{p,q}\underline{A}_{pq}^{(i)}\sin\left(\frac{p\pi}{L_{px}}x\right)\sin\left(\frac{q\pi}{L_{py}}y\right), \quad (17)$$

with p, q = 1,2,3,.... These expansion functions satisfy *a priori* the simply supported boundary conditions.

The forces and moments in each line connection are also written as an expansion series:

$$\underline{\hat{F}}_{\mathrm{l}i}^{(1)/(2)} = \sum_q \underline{F}_{\mathrm{l}i,q}^{(1)/(2)}\sin\left(\frac{q\pi}{L_{py}}y\right), \quad (18)$$

$$\underline{\hat{M}}_{\mathrm{l}i}^{(1)/(2)} = \sum_q \underline{M}_{\mathrm{l}i,q}^{(1)/(2)}\sin\left(\frac{q\pi}{L_{py}}y\right). \quad (19)$$

The beam displacements are expanded as:

$$\underline{\hat{w}}_{\mathrm{b}zi} = \sum_q \underline{w}_{\mathrm{b}zi,q}\sin\left(\frac{q\pi}{L_{py}}y\right), \quad (20)$$

$$\underline{\hat{\theta}}_{\mathrm{b}yi} = \sum_q \underline{\theta}_{\mathrm{b}yi,q}\sin\left(\frac{q\pi}{L_{py}}y\right). \quad (21)$$

2.3. Boundary and continuity conditions

At the rigid back walls of source and receiving room, the air particle displacement must be zero:

$$\underline{\hat{w}}_a^{(0)}(x,y,0) = 0, \quad (22)$$

$$\underline{\hat{w}}_a^{(3)}(x,y,L_z^{(N+1)}) = 0. \quad (23)$$

At the plates surfaces, continuity of transverse displacement is imposed,

$$\underline{\hat{w}}_a^{(1)}(x,y,L_z^{(1)}) = \underline{\hat{w}}_p^{(1)}(x,y) = \underline{\hat{w}}_a^{(2)}(x,y,0), \quad (24)$$

$$\underline{\hat{w}}_a^{(2)}(x,y,L_z^{(2)}) = \underline{\hat{w}}_p^{(2)}(x,y) = \underline{\hat{w}}_a^{(3)}(x,y,0). \quad (25)$$

For the case of beams coupling the two plates, continuity of transverse displacement and rotation is imposed,

$$\underline{\hat{w}}_p^{(1)}(x_{\mathrm{s}i},y) = \underline{\hat{w}}_{\mathrm{b}zi}(y) = \underline{\hat{w}}_p^{(2)}(x_{\mathrm{s}i},y), \quad (26)$$

$$\frac{\partial\underline{\hat{w}}_p^{(1)}(x_{\mathrm{s}i},y)}{\partial x} = \underline{\hat{\theta}}_{\mathrm{b}yi}(y) = \frac{\partial\underline{\hat{w}}_p^{(2)}(x_{\mathrm{s}i},y)}{\partial x}. \quad (27)$$

2.4. Construction of system matrices and post-processing

Because the proposed pressure expansions are exact solutions of the homogeneous Helmholtz equation, the participation factors $\underline{P}_{mn}^{(i)}$ and $\underline{Q}_{mn}^{(i)}$ are only determined by the boundary and continuity conditions. The pressure expansion functions satisfy *a priori* the rigid wall boundary conditions. The other boundary and continuity conditions can only be satisfied approximately, as only a finite number of expansion functions can be taken into account. The residuals on

the boundaries are minimized in an integral sense using a Galerkin weighted residual formulation [9]. The wave functions used in the field variable expansions are used as weighting functions. Because of the rectangular geometry, the factors $\underline{P}_{mn}^{(i)}$ and $\underline{Q}_{mn}^{(i)}$ can be eliminated analytically in function of the unknowns $\underline{A}_{pq}^{(i)}$ by use of the weighted residual formulation of the boundary and continuity conditions (22)-(25). Equations (11) and (12) for the plates, equations (6) and (7) for the beams, and equations (3)-(5) for the spring connections are also solved by means of a weighted residual formulation. This results in a symmetric set of linear equations in the primary unknowns $\underline{A}_{pq}^{(i)}$, $\underline{F}_{\mathrm{s}i}$, $\underline{F}_{\mathrm{l}i,q}^{(1)/(2)}$, $\underline{M}_{\mathrm{l}i,q}^{(1)/(2)}$, $\underline{w}_{\mathrm{b}zi,q}$ and $\underline{\theta}_{\mathrm{b}yi,q}$.

The additional computational effort to include structural connections in the wave based model is limited, because the structural connections do not influence the original matrix elements for the double wall model without structural connections; it only results in additional columns and rows.

After the wave function contribution factors are determined, the transmission loss (TL) is determined by following measurement formula:

$$\mathrm{TL} = L_{pe} - L_{pr} + 10\log\frac{S}{A_r}, \tag{28}$$

where L_{pe} and L_{pr} are the average sound pressure level in emitting and receiving room, S is the surface area of the wall and $A_r = \frac{0.16V_r}{T_r}$ the absorption area of the receiving room, with V_r the volume and T_r the reverberation time. Calculations are performed at 81 frequencies per one-third octave band and averaged.

3. Results

3.1. Wooden floor

As a first example a wooden floor is considered, consisting of 25 mm matched boards in floor and ceiling. The boards are coupled by wooden beams with height 220 mm (equal to the cavity depth), width 67 mm and spacing distance 600 mm. The cavity is filled with mineral wool with a flow resistivity of 17700 Ns/m^4.

First, the wooden beams are modeled as rigid line connections. The TL of the wooden floor is calculated with the decoupled approach of Davy [5], the periodic model of Legault *et al.* [8] and the WBM. In the WBM, a floor with dimensions 4 m × 3 m is considered with seven 3 m long beams. The material properties used for the wooden floor and ceiling boards are given in table I. The mineral wool is modeled as an equivalent fluid. The results are shown in figure 2 and compared with the TL of the infinite floor without structural connections as calculated with the transfer matrix method. The rigid line connections influence the TL in the entire frequency range of interest. All models show that the structure-borne sound transmission is dominant above 63 Hz. Around 630 − 800 Hz,

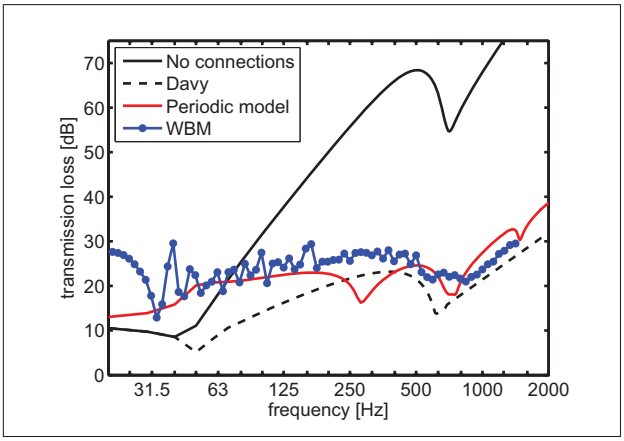

Figure 2. TL of a double wooden floor without and with rigid line connections.

Table I. Material properties used in simulations.

	ρ [kg/m^3]	E [MPa]	η [-]	ν [-]
Wood (plate)	500	6550	0.01	0.30
Wood (beam)	500	9800	0.015	0.30
Aluminum	2742	70000	0.01	0.33
Gypsum	720	2500	0.03	0.30

the coincidence dip of the wooden boards is observed. The periodic model predicts two additional dips at 280 Hz and 1500 Hz linked to the pass bands of the periodic structure. This pass- and stop-band behaviour is not seen for the finite plate with seven beams. Below 200 Hz, the WBM fluctuations reflect the modal behaviour of the finite structure, but the general trends are the same as for the periodic model. The studs improve the TL below 63 Hz thanks to the increased stiffness. This cannot be predicted with the model of Davy, because the total transmission is calculated as the sum of the airborne and structure-borne transmission component. Furthermore, the semi-analytical approach of Davy disregards any pass- and stop-band phenomena caused by wave propagation in the periodic structure.

When the beams are modeled as separate elements in the WBM (section 2.1.3), the TL is slightly changed (figure 3). Above 50 Hz, the TL is increased by approximately 3 dB in most frequency bands thanks to the additional mass of the wooden beams. At low frequencies, the positive influence of the stiffness of the rigid connections is not observed any more when taking into account the modal behaviour of the beams.

3.2. Aluminum double panel

A second example considers the double aluminum panel of [8]. It is made up from two 1220 mm × 2030 mm aluminum plates with thickness 1 and 2 mm separated by a 50.8 mm cavity filled with a fibrous material. The aluminum panels, with material properties given in table I, are linked with five C-section

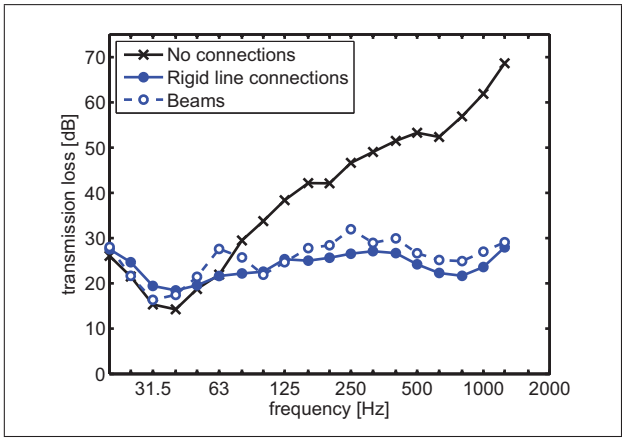

Figure 3. WBM simulations of the TL (in 1/3 octave bands) of a 4 m × 3 m double wooden floor without and with wooden beams.

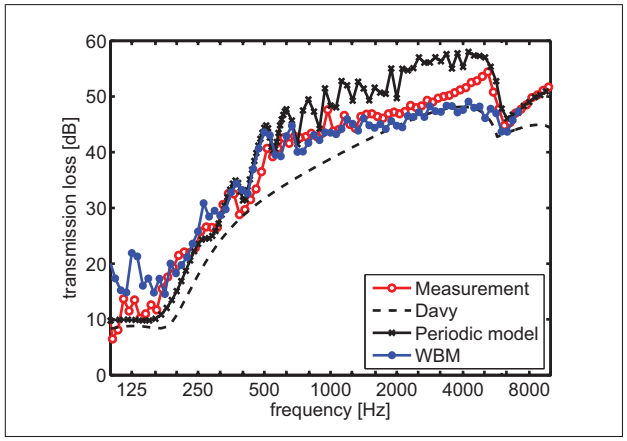

Figure 4. Measured and simulated TL (taken from [8]) of an aluminum double panel with 5 C-section channels.

aluminum channels spaced by a distance of 508 mm. The TL of the double panel is predicted with the WBM and with the infinite plate models of Davy [5] and Legault *et al.* [8]. The channels are modeled as line connections with a translational stiffness $K'_t = 22.8 \times 10^6\,\mathrm{N/m^2}$ and a rotational stiffness $K'_r = 3.675 \times 10^3\,\mathrm{Nm/rad\,m}$, as suggested in [8].

Figure 4 compares the measured 1/12 octave band TL [8] with the different simulation results. The decoupled model of Davy underestimates the TL in the entire frequency range of interest. The periodic model gives good agreement up till 500 Hz. In the frequency range 630 − 5000 Hz, where the TL is dominated by structure-borne sound transmission across the channels, the TL is overestimated by 5 to 10 dB. The coincidence dip at 6300 Hz is well predicted. The WBM results correspond well with the measured TL in a broad frequency range with only an underestimation around 4000 Hz. The overestimation at low frequencies can be attributed to the fact that no detailed information was available on the measurement setup and transmission rooms, making assumptions necessary in the WBM. Again, the pass- and stop-band behaviour predicted with the periodic model is not observed as clearly in the WBM and measurement results.

3.3. Double gypsum fiberboard wall

Finally, a double gypsum plasterboard wall with cavity thickness 45 mm and 12.5 mm thick leafs is considered. The cavity is filled with a 40 mm mineral wool layer. The TL was measured in the large transmission opening of the reverberation chambers of the Laboratory of Acoustics at the KU Leuven. The transmission opening has a width of 3.25 m and a height of 2.95 m. The leafs are screwed to a steel stud frame consisting of 5 steel studs type CW with a spacing of 60 cm. The distance between screws is 25 cm.

The TL is simulated the WBM. The material properties used for the gypsum plasterboard leafs are given in table I. The mineral wool is modeled as an equivalent fluid assuming a flow resistivity of 10000 Ns/m^4. The steel studs are modeled as:

- rigid line connections;
- line connections with a frequency dependent, equivalent translational stiffness $K'_{\mathrm{ts}}(f)$ according to [12, 13]:

$$\log K'_{\mathrm{ts}} = 0.6286x^3 - 4.4051x^2 + 10.3323x - 2.0722 \quad \text{with} \quad x = \log f; \tag{29}$$

- 12 rigid point connections with spacing distance $d_{\mathrm{s}} = 25$ cm;
- 4 rigid point connections with spacing distance $d_{\mathrm{s}} = 75$ cm;

The last cases are included to investigate whether the assumption of a perfect line connection is reasonable, knowing that the panels and studs are only fixed at discrete positions. A reference model without steel studs is also set up.

The WBM results are compared with the measured TL in figure 5. In the frequency range 125−250 Hz, the WBM without structural connections agrees well with the measurement results, indicating that the airborne transmission is dominant in this frequency range. However, the TL is underestimated below 125 Hz and overestimated above 250 Hz. The studs improve the TL at low frequencies. The largest improvement is found when the studs are modeled as rigid line connections, but the difference between all models is small. Above 250 Hz, structure-borne sound transmission is important. In this frequency range, the TL is therefore strongly influenced by the type of structural coupling. When the studs are modeled as rigid line connections, the structure-borne sound transmission is overestimated and the overall TL is underestimated. The equivalent translational spring model gives better results above 315 Hz, but underestimates the TL strongly around 250 Hz. The models with rigid point connections give a higher TL than the model with rigid line connections, apart from a strong dip at

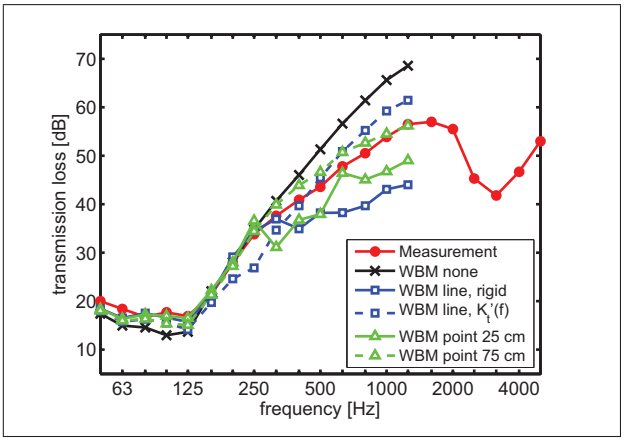

Figure 5. TL of a double gypsum fiberboard wall 12.5 / 45 / 12.5 mm with steel studs and cavity absorption. Experimental results and WBM simulations.

315 Hz in the model with 12 rigid point connections ($d_s = 25$ cm). The TL increases significantly when the number of point connections is reduced. Generally, the model with point connections with $d_s = 75$ cm agrees best with the measurement results. These results indicate, however, that it is difficult to accurately predict the TL in this frequency because the structure-borne sound transmission can be influenced by small details. The importance of small details has also been observed in experiments [1] and round robin tests [14]. The loss factor of the plates, which was estimated in the model, may also influence the TL significantly [9].

4. Conclusions

In this paper, the wave based methodology is extended for the investigation of the sound transmission through double walls with structural connections. Comparison between WBM results and infinite plate results show that the finite dimensions can have a significant influence on the sound insulation, both at low frequencies and at higher frequencies. Some general trends are observed in the WBM simulations. At and below the mass-spring-mass resonance frequency, the TL is improved thanks to the stiffness provided by the studs. At mid frequencies, the TL is determined by airborne transmission through the cavity and the influence of structural connections is limited. For double walls with cavity absorption, the structure-borne transmission is dominant above a certain bridge frequency, which is determined by the specific configuration of the double wall and the structural connections. In this frequency range, the TL is influenced by the type of structural coupling (point or line connections, rigid, spring or beam connections), making accurate predictions difficult in building acoustical applications. The pass- and stop-band behaviour observed for infinite periodic structures cannot fully develop in finite double walls.

Acknowledgement

Arne Dijckmans is a postdoctoral fellow of the Research Foundation Flanders (FWO). This research was performed within a research stay at the Acoustics Research Unit (Liverpool), funded by the FWO. The financial support is gratefully acknowledged.

References

[1] V. Hongisto, M. Lindgren, R. Helenius, Sound insulation of double walls – An experimental parametric study, Acta Acust. united Ac. 88 (6) (2002) 904–923.

[2] R. Craik, Sound Transmission through Buildings using Statistical Energy Analysis, Gower, England, 1996.

[3] B. Sharp, Prediction methods for the sound transmission of building elements, Noise Control Eng. J. 11 (1978) 53–63.

[4] F. Fahy, P. Gardonio, Sound and structural vibration, 2nd edition: Radiation, transmission and response, Academic Press, 2007.

[5] J. Davy, Sound transmission of cavity walls due to structure borne transmission via point and line connections, J. Acoust. Soc. Am. 132 (2) (2012) 814–821.

[6] G.-F. Lin, J. Garrelick, Sound transmission through periodically framed parallel plates, J. Acoust. Soc. Am. 61 (4) (1977) 1014–1018.

[7] J. Brunskog, P. Hammer, Prediction model for the impact sound level of lightweight floors, Acta Acust. united Ac. 89 (2) (2003) 309–322.

[8] J. Legault, N. Atalla, Numerical and experimental investigation of the effect of structural links on the sound transmission of a lightweight double panel structure, J. Sound Vib. 324 (3-5) (2009) 712–732.

[9] A. Dijckmans, G. Vermeir, W. Lauriks, Sound transmission through finite lightweight multilayered structures with thin air layers, J. Acoust. Soc. Am. 128 (6) (2010) 3513–3524.

[10] C. Díaz-Cereceda, J. Hetherington, J. Poblet-Puig, A. Rodríguez-Ferran, A determinisctic model of impact noise transmission through structural connections based on modal analysis, J. Sound Vib. 330 (12) (2011) 2801–2817.

[11] A. Arjunan, C. Wang, K. Yahiaoui, D. Mynors, T. Morgan, V. Nguyen, M. English, Finite element acoustic analysis of a steel stud based double-leaf wall, J. Sound Vib. 333 (23) (2014) 6140–6155.

[12] J. Poblet-Puig, A. Rodríguez-Ferran, C. Guigou-Carter, M. Villot, The role of studs in the sound transmission of double walls, Acta Acust. united Ac. 95 (3) (2009) 555–567.

[13] J. Davy, C. Guigou-Carter, M. Villot, An empirical model for the equivalent translational compliance of steel studs, J. Acoust. Soc. Am. 131 (6) (2012) 4615–4624.

[14] P. Fausti, R. Pompoli, R. Smith, An intercomparison of laboratory measurements of airborne sound insulation of lightweight plasterboard walls, Building Acoustics 6 (2) (1999) 127–140.